X-ray spectral analysis of the microquasar 1E 1740.7-2942

E.A. Saavedra[1], P. Sotomayor Checa[1,2], F.L. Vieyro[1,2] & G.E. Romero[1,2]

[1] Facultad de Ciencias Astronómicas y Geofísicas, UNLP, Argentina
[2] Instituto Argentino de Radioastronomía, CONICET–CIPCPBA–UNLP, Argentina

Contact / saavedraenz@gmail.com

Resumen / Presentamos los resultados de un estudio de la emisión de rayos X del microquasar 1E1740.7-2942, conocido como *"el Gran Aniquilador"*. La observación fue realizada el 14 de mayo del 2021 y tiene una duración de 44 ks. El análisis temporal mostró un comportamiento de baja variabilidad alrededor de 12.57 ± 0.64 c/s. El análisis espectral muestra que con un modelo tipo ley de potencias más un cuerpo negro es suficiente para poder describir el espectro. El índice de la ley de potencias ($E^{-\Gamma}$) es de $\Gamma \approx 1.8$ y la temperatura asociada al cuerpo negro es de ≈ 0.3 keV. Proponemos una interpretación del espectro basada en un jet relativista y una corona caliente, e inferimos los correspondientes parámetros físicos.

Abstract / We present the results of the study of the X-ray emission of the microquasar 1E1740.7-2942, known as "the Great Annihilator". The observation was made on 14 May 2021 and had a duration of 44 ks. The temporal analysis shows a low variability behaviour around 12.57 ± 0.64 c/s. The spectral analysis indicates that a power-law model plus a blackbody is sufficient to describe the spectrum. The power-law index ($E^{-\Gamma}$) is $\Gamma \approx 1.8$ and the associated blackbody temperature is ≈ 0.3 keV. We propose an interpretation of the spectrum based on a relativistic jet and a hot corona, and infer the corresponding physical parameters.

Keywords / stars: individual (1E 1740.7-2942) — stars: black holes — stars: jets — X-rays: binaries — relativistic processes — accretion, accretion disks

1. Introduction

The astrophysical source 1E 1740.7-2942 is the brightest hard X–ray source near the Galactic Center. The source was discovered with the *Einstein Observatory* satellite (Hertz & Grindlay, 1984), and classified as a black hole candidate because of its similarities with Cygnus X–1 (Sunyaev et al., 1991). When a double sided radio emitting jet associated with the source was discovered by Mirabel et al. (1992), the source was classified as a *"microquasar"*. The system was later classified as a high-mass X-ray binary system with a black hole, due to the detection of an extended near-infrared counterpart (Martí et al., 2010). No optical or infrared counterpart are detected since the system suffers from extremely high galactic extinction (e.g., Gallo et al. 2003).

The source spends most of the time in the low/hard state (LHS), as observed by different telescopes over the years (del Santo et al. 2005; Reynolds & Miller 2010; Natalucci et al. 2014a). This state can be well described by a thermal comptonisation model (Castro et al., 2014; Stecchini et al., 2021). Bosch-Ramon et al. (2006) applied a jet+corona model to study the multiwavelenght behavior of the source. In this work, we aim at analyzing the new X-ray observations of the source, and apply a similar jet-corona model to account for the new data.

2. Observation and Data Analysis

NuSTAR (*Nuclear Spectroscopic Telescope Array*; Harrison et al. 2013) observed 1E 1740.7-2942 with its two co-aligned telescopes operating in the 3–79 keV energy range; each telescope has its own Focal Plane Module, A (*FPMA*) and B (*FPMB*), consisting of a solid-state CdZnTe solid-state detector. 1E 1740.7-2942 was observed in May 14, 2021 (ObsID 90701317002), with an exposure of 44 ks and livetime of 23.6 ks. The data were reduced using NuSTARDAS-v. 2.0.0 analysis software from the HEASoft v.6.28 task package and CALDB (V.1.0.2) calibration files. The source events collected within a circular region of 119 arcsecond radius around the focal point. Background events were taken from a source-free circular region with a radius of 164 arcseconds.

Light curves and spectra were extracted using nuproducts task. Background light curve subtraction and addition of the light curves of both detectors was performed by the LCMATH task. We corrected observations folded to obtain a final light curve.

XSPEC v12.11.1 package (Arnaud, 1996) was employed to model the spectra. The source spectrum were rebinned to have at least 30 counts per energy bin, in the 3–79 keV energy band, in order to apply χ^2 statistics. In order to analyze the spectral properties of the source, average and time resolved spectra were extracted for each camera.

3. Results

3.1. Timing analysis

In Fig. 1 we show a light curve of the source with a binning of 100 s in the 3–79 keV energy range. A statistical analysis of the light curve was performed using the
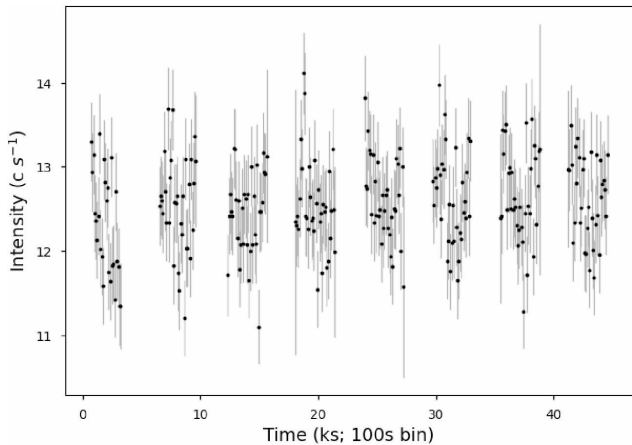
Poster contribution

Figure 1: Background corrected light curve of 1E 1740.7-2942 with a binning of 100 s, starting at 59348.4244 MJD.
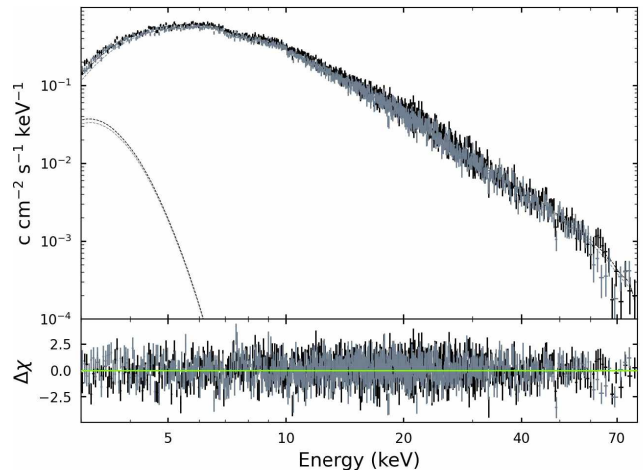

Figure 2: *Top panel:* NuSTAR's FPMA and FPMB average energy spectrum of 1E 1740.7-2942. The continuum can be described by a contribution of absorbed powerlaw and blackbody. *Bottom panel:* residuals associated with the continuous model.

`lcstats` task. An average of 12.57 c/s with a standard deviation of 0.64 c/s was found.

Light curves with different time binning were extracted. All of them showed a constant behavior around an average value. The `powspec` task was used to search for oscillations such that the Nysquit frequency was 715 Hz in the power spectrum. No significant oscillations were found.

3.2. Spectral analysis

A spatially resolved spectral analysis was performed in order to characterize the source. Simultaneous modelling of the source and the background were performed using the two NuSTAR telescopes in which the calibration counter varied by 2%.

The broadband spectrum of the source can be adequately fitted by means of a composite model with two continuum components: a black body model, with its peak at low energies, and a power law. The region associated with low energies was tested with the `bbody` and `diskbb` models, due to the fact that residuals when fitting a continuous component showed excess counts around ≈ 3 keV. For the `diskbb` model there was no way to fit, as in all cases the T_{in} or normalization errors diverged. The best fit was obtained with a `bbody` at ≈ 0.3 keV.

The interstellar absorption was modelled using the Tuebingen-Boulder interstellar absorption model (`tbabs`), with solar abundances set according to Wilms et al. (2000), and the effective cross sections given by Verner et al. (1996).

The parameters associated with the best-fit final model and the spectrum are given in Table 1 and Figure 2, respectively.

3.3. Broadband spectrum modelling

A stationary one-zone relativistic conical jet model was used to model the jet emission. We consider that electrons are cooled by synchrotron radiation, inverse Compton scattering against photons from the accre-

Parameters	Values
$C_{FPMA/FPMB}$	1.020 ± 0.007
$n_H (\, 10^{22} \text{ cm}^{-2})$	11.9 ± 0.3
Γ	1.85 ± 0.01
norm	0.077 ± 0.004
kT_{BB} (keV)	0.29 ± 0.06
norm	0.010 ± 0.006
χ^2/dof	$1384.68/1350$

Table 1: Final parameters of the energy spectrum in the 3–79 keV range of the `const*tbabs*(powerlaw+bbody)`.

tion disc and synchrotron-self Compton, relativistic Bremsstrahlung, adiabatic losses by the lateral expansion of the jet, and they can escape from the acceleration region by advection. The transport equation was solved numerically and the calculated fluxes were transformed to the observer reference frame. We explore the parameter space to determine whether the jet model is sufficient to simultaneously explain the radio and X-ray data. We add the thermal emission generated by a corona above the accretion disc considering a power-law distribution with an exponential cutoff.

When applying a single jet model, we find that although the synchrotron emission of the jet can fit the X–ray data, it is not adequate to model the radio data by several orders of magnitude. A jet two-zone model can explain both bands simultaneously. Alternatively, when applying a combined jet+corona model, we are able to reproduce all components: the jet is responsible for the radio flow, and a corona for the NuSTAR data. The best-fit parameters and the associated SED can be seen in Table 2 and Fig. 3. Jet parameters are consistent with those considered in Bosch-Ramon et al. (2006). In particular, the acceleration region is located in the range of the spatial resolution of the instrument.
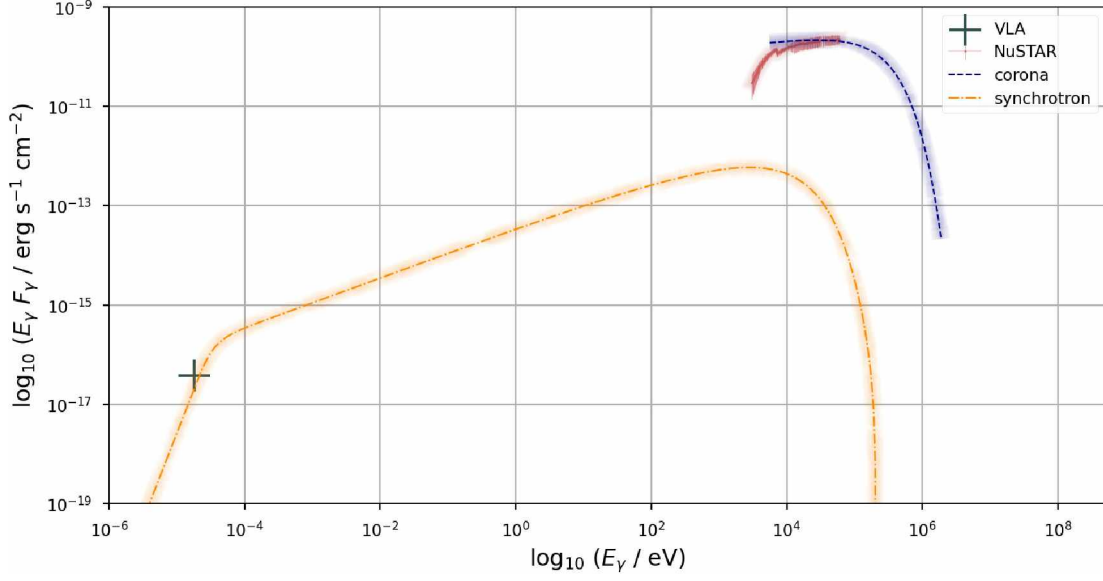
Figure 3: Spectral energy distribution associated with the source 1E 1740.7-2942. Two models were fitted to explain the observations associated with the radio band and the X-ray band. The model associated with a relativistic jet is shown in green, and a thermal corona in white. Only the SED components relevant for the fit are shown.

Jet Parameters	Coronal Parameters
$L_k = 5 \times 10^{37}\,\mathrm{erg\,s^{-1}}$	$M_{bh} = 5 M_\odot$
$\Gamma_j = 1.035$	$Rc = 7.38 \times 10^7$ cm
$z_0 = 200\,\mathrm{r_g}$	$T_e = 1 \times 10^9$ K
$z_{acc} = 9 \times 10^5\,\mathrm{r_g}$	$T_i = 1 \times 10^{12}$ K
$B_0 = 8.7 \times 10^6$ G	$B_{mag} = 2.7 \times 10^5$ G
$B_{acc} = 0.4$ G	$n_i = 1.40 \times 10^{13}\,\mathrm{cm^{-3}}$
$q_{rel} = 0.1$	$n_e = 1.40 \times 10^{13}\,\mathrm{cm^{-3}}$
$p = 2$	$\Gamma = 1.85$
$\eta_{acc} = 10^{-3}$	$\Gamma_{cutoff} = 190$ keV

Table 2: Parameters adopted in the jet model: L_k is the kinetic power, Γ_j is its Lorentz factor, z_0 is the launch point, z_{acc} is the relativistic particle injection point, $\mathrm{r_g} = GM_{bh}/c^2$ is the gravitational radius, B_0 is the magnetic field at z_0, B_{acc} is the magnetic fild at z_{acc}, q_{rel} is the fraction of the jet power in relativistic particles, p is the injection spectral index and η_{acc} is the acceleration efficiency. Parameters adopted in the corona model: M_{bh} is the black hole mass, Rc is the corona radius, T_e is the electron temperature, T_i is the ion temperature, B_{mag} is the magnetic field, n_i and n_e are plasma density, Γ is the x-ray spectrum power-law index and Γ_{cutoff} is the x-ray spectrum cut-off (Natalucci et al., 2014b).

4. Conclusions

The reduction of the recent NuSTAR observation and its subsequent analysis allowed us to infer some parameters of the microquasar 1E1740.7-2942. In order to reproduce the SED, we applied a relativistic jet model and a thermal corona model. We show that a one-zone jet model is not sufficient to explain the X-ray observations. This is in agreement with the results in Bosch-Ramon et al. (2006).

In the future, a hadronic component will be added to the jet model and non-thermal processes in the corona. Observations in different spectral bands will also be added to test the proposed models more robustly.

References

Arnaud K.A., 1996, G.H. Jacoby, J. Barnes (Eds.), *Astronomical Data Analysis Software and Systems V, Astronomical Society of the Pacific Conference Series*, vol. 101, 17

Bosch-Ramon V., et al., 2006, A&A, 457, 1011

Castro M., et al., 2014, A&A, 569, A82

del Santo M., et al., 2005, A&A, 433, 613

Gallo E., Fender R.P., Pooley G.G., 2003, MNRAS, 344, 60

Harrison F.A., et al., 2013, ApJ, 770, 103

Hertz P., Grindlay J.E., 1984, ApJ, 278, 137

Martí J., et al., 2010, ApJL, 721, L126

Mirabel I.F., et al., 1992, Nature, 358, 215

Natalucci L., et al., 2014a, ApJ, 780, 63

Natalucci L., et al., 2014b, ApJ, 780, 63

Reynolds M., Miller J., 2010, ApJ, 716

Stecchini P.E., et al., 2021, Astron. Nachr., 342, 315

Sunyaev R., et al., 1991, ApJL, 383, L49

Verner D.A., et al., 1996, ApJ, 465, 487

Wilms J., Allen A., McCray R., 2000, ApJ, 542, 914